Virology 468-470 (2014) 592–600

Contents lists available at ScienceDirect

Virology

journal homepage: www.elsevier.com/locate/yviro

# Enterovirus 71 infects brain-derived neural progenitor cells

Hsing-I Huang [a,b,*,1], Jhao-Yin Lin [a,c,1], Hsin-Hsu Chen [a,b], Shiou-Bang Yeh [b], Rei-Lin Kuo [a,b], Kuo-Feng Weng [a], Shin-Ru Shih [a,b,d]

[a] Department of Medical Biotechnology and Laboratory Science, Research Center for Emerging Viral Infections, Chang Gung University, 259 Wen-Hwa 1st Road, Kwei-Shan, Tao-Yuan, Taiwan, ROC
[b] Department of Medical Biotechnology and Laboratory Science, College of Medicine, Chang Gung University, Kwei-Shan, Tao-Yuan, Taiwan, ROC
[c] Graduate institute of Biomedical Sciences, Chang Gung University, Kwei-Shan, Tao-Yuan, Taiwan, ROC
[d] Clinical Virology Lab, Department of Clinical Pathology, Chang Gung Memorial Hospital, Kwei-Shan, Tao-Yuan, Taiwan, ROC

ARTICLE INFO

*Article history:*
Received 26 June 2014
Returned to author for revisions
17 July 2014
Accepted 17 September 2014
Available online 6 October 2014

*Keywords:*
Neural progenitor cells
EV71
Permissiveness

ABSTRACT

Neural progenitor cells (NPCs) are stem cells that can differentiate into various neural lineage cells. The damage and loss of NPCs are associated with neurological conditions such as cognitive deficits and memory impairment. In a long-term study of patients with EV71, cognitive disorders were observed. Therefore, we hypothesized that NPCs may be permissive to EV71 infection. We demonstrated that NPCs are prone to EV71 infection and that these stem cells can support the active replication of this virus. Furthermore, EV71 infection triggers apoptosis, resulting in significant cell death in infected NPCs. However, EV71 did not replicate in the differentiated cell types that were tested. Our findings suggest that EV71 can infect NPCs and cause the depletion of these cells.



## Introduction

EV71 is a member of the *Picornaviridae* family. Frequent EV71 epidemics have been observed in the Asia-Pacific region since this virus was first identified in 1969 in California, United States (Schmidt et al., 1974). In most cases, mild symptoms, such as herpangina and hand-foot-and-mouth disease, have been recorded; however, serious neurological complications may occur in young children (Wang et al., 1999, 2011; Chang et al., 2002). Once EV71 invades the central nervous system (CNS), the consequent pathological conditions may include aseptic meningitis, flaccid paralysis, Guillain–Barré syndrome, transverse myelitis, cerebellar ataxia, brainstem encephalitis and pulmonary edema (Melnick, 1984; Chen et al., 2001; McMinn, 2002). Although the induced neurological diseases account for the mortality and severity of EV71 infection, the pathogenesis of EV71-associated neurological disorders has not been completely elucidated.

Neural progenitor cells (NPCs) are capable of self-renewal and can differentiate into neural lineage cells. These cells play key roles in neurodevelopment and in repairing damage to the nervous system (Mckay, 1997). Previous studies of NPCs have investigated their differentiation potential and their possible application in regenerative medicine (Su and Vellis, 2009). Recent studies have shown that lesions of neural progenitor cells are correlated with long-term neuropathological symptoms, including learning and recognitive defectives (Haughey et al., 2002; Kim et al., 2008). Furthermore, several pathogens trigger the death of neural progenitors *via* primary infection or secondary effects and thus result in neurofunctional deficits (Hofer et al., 2011).

Several neurotrophic viruses such as Borna disease virus (BDV), Japanese encephalitis virus (JEV), and cytomegalovirus (CMV) have been shown to cause behavioral changes and recognition and learning deficits in infected patients (Das and Basu, 2008; Cheeran et al., 2005; Briese et al., 1999). These viruses are able to infect neural progenitors and thus affect the differentiation, proliferation and lifespan of these cells, resulting in impaired neurogenesis and long-term deficits (Ariff et al., 2013; Brnic et al., 2012; Odeberg et al., 2006, 2007). Therefore, we hypothesized that the long-term abnormalities following EV71 infection may be due to the effects of the virus on the neural progenitor cells.

In the present study, we infected mice with EV71 and examined whether NPCs could be affected. We show that EV71 could be detected in the NPCs residing in the brain. Furthermore, isolated NPCs were used to investigate the effects of EV71 infection. EV71 infection induces robust cell death in NPCs, which may result in the depletion of the NPC pool. In contrast with the NPCs, differentiated neuronal cells and astrocytes cells are less permissive to EV71 infection. Therefore, the results of this study suggest that NPCs can support EV71 replication in the brain, and that EV71 infection results in the loss of NPCs.

* Corresponding author at: Department of Medical Biotechnology and Laboratory Science, Research Center for Emerging Viral Infections, Chang Gung University, 259, Wen-Hwa 1st Road, Kwei-Shan, Tao-Yuan 333, Taiwan, ROC. Fax: +886 3 2118700.
*E-mail address:* hihuang@mail.cgu.edu.tw (H.-I. Huang).
[1] These authors contributed equally to this article.

http://dx.doi.org/10.1016/j.virol.2014.09.017
0042-6822/

## Results

### *Detection of EV71-infected cells in the mouse brain*

To test whether EV71 could infect NPCs *in vivo*, animal experiments were performed. For these experiments, 5-day-old neonatal mice were intraperitoneally administered $5 \times 10^5$ pfu of EV71 strain 4643 MP4. At 24 and 48 h post-infection, the mice were sacrificed, and the brain tissue was collected for analysis. Sagittal brain sections were obtained, and staining with an anti-EV71 Ab revealed that EV71 was distributed in the hippocampus, the subventricular zone (SVZ), and the lining of the lateral ventricle (Fig. 1A). The presence of NPCs was then detected by nestin expression (Lendahl et al., 1990). An anti-nestin Ab was used to detect undifferentiated NPCs. Double immunofluorescence staining showed that many nestin-positive cells were infected by EV71 (Fig. 1B).

### *Mouse NPCs are permissive to infection by mouse-adapted EV71*

NPCs were isolated and expanded. These cells were grown as monolayers in culture vessels (Supplementary Fig. 1A). We tested various differentiation protocols. Differentiation was confirmed by the expression of specific cell markers. Microtubule-associated protein 2 (MAP2) was used as the marker for differentiated neuronal cells, whereas glial fibrillary acidic protein (GFAP) was the marker for astrocyte lineage cells. Nestin was expressed by all of the isolated neural progenitor cells, whereas GFAP and MAP2 were absent.

We first tested the infectivities of the clinically isolated strain EV71 4643 and the mouse-adapted strain EV71 4643 MP4 in NPCs. The cells were seeded in 12-well plates and infected with these two strains at an MOI of 40. Cytopathic effects could be observed as early as 12 h in the cells that were infected with the EV71 4643 MP4

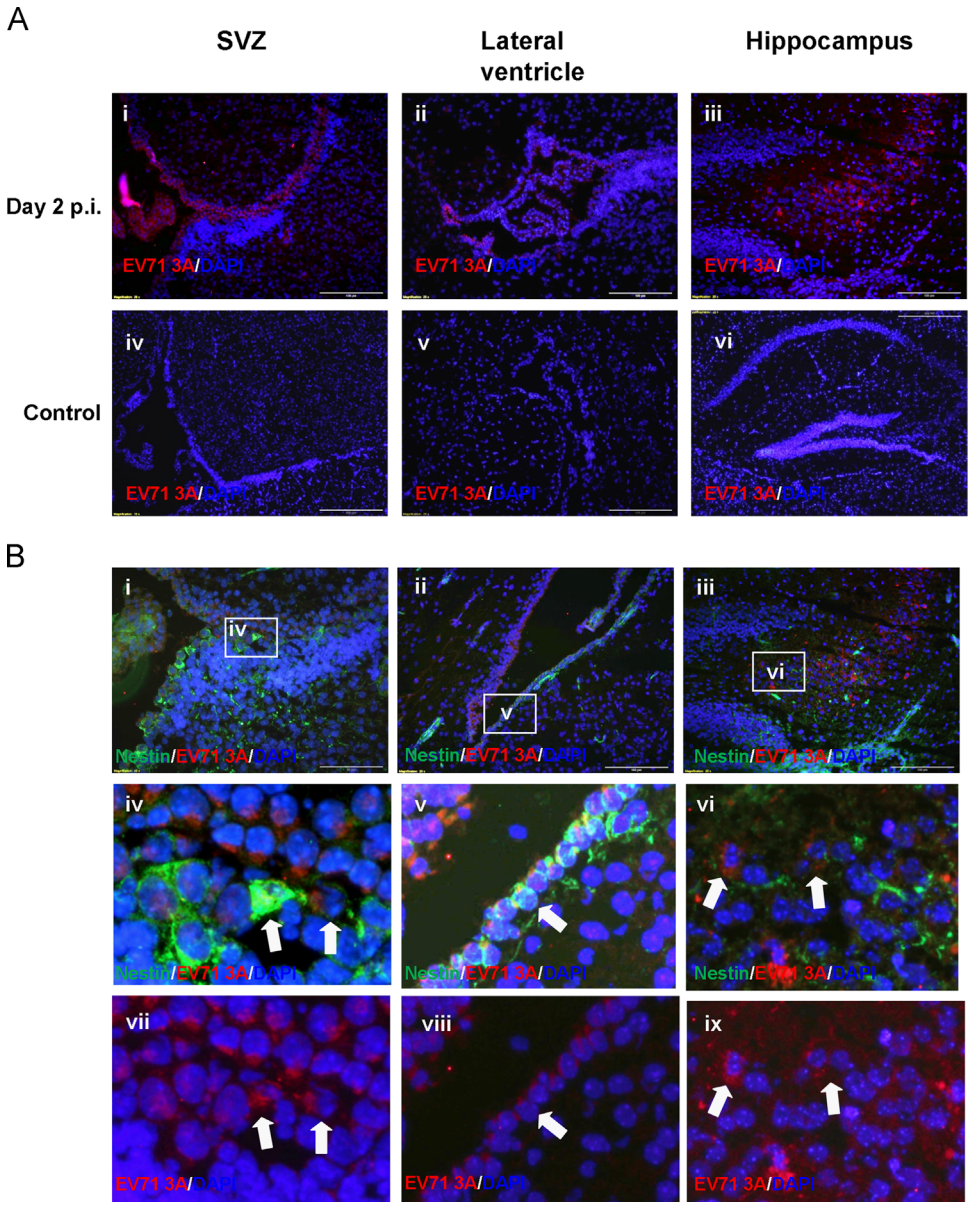


**Fig. 1.** Distribution of EV71 antigen in the mouse brain. (A) Cryostat sections prepared from brain of EV71 infected mouse pups were stained with anti-EV71 3A antibody. Expression of EV71 antigen was observed in different sections of brain. EV71 Infected cells were evident in the subventricular zone (A-i), the lining of lateral ventricles (A-ii), and the hippocampus, (A-iii). Mocked-infected mouse were injected with medium alone. The brain sections of control group were shown in A-iv-A-v-A-vi immunofluresence staining was performed by using anti-EV71 3A antibodies and anti-nestin antibodies. PE-conjugated anti-rabbit IgG and FITC-conjugated anti-mouse IgG secondary antibodies were used for detection. Nestin positive (green) cells were observed and some of these cells were infected by EV71 (red) (B-i–B-iii). A higher magnification of this area (white box) is shown (B-iv–Bix). A-iv, A-vi, 10× objective; A-i, A-ii, A-iii, A-v, B-ii, B-iii, 20× objective; B-i, 40× objective; B-v, B-vi, B-viii, B-ix, 20× objective with additional fivefold computer-generated magnification. B-iv, B-vii 40× objective with additional fivefold computer-generated magnification. The white arrows indicated that the cells were positive stained with anti-nestin and anti-EV71 3A antibodies.

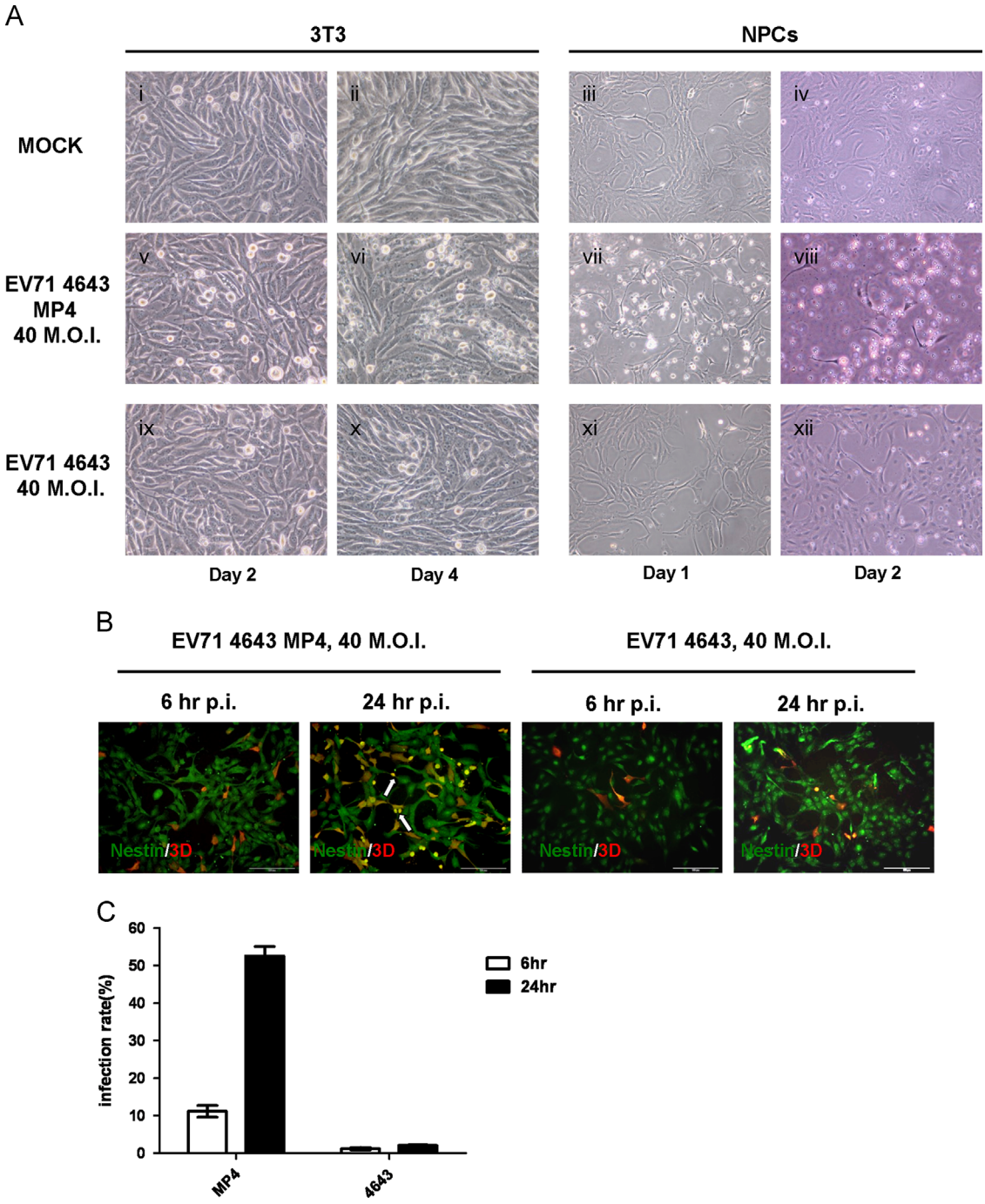


**Fig. 2.** NPCs and 3T3 cells are permissive for EV71 infection. (A) EV71 MP4 infection causes cytopathic effects in 3T3 and NPCs. 3T3 and NPCs were expanded and seeded in 6-well plates. The seeded cells were mock inoculated (i–iv) or infected with EV71 4643 MP4 (v–viii) or EV 4643 (ix–xii) at an M.O.I. of 40. The morphological changes were observed daily to assess the cytopathic effects. (3T3 cells, magnification = 400 × ; NPCs, magnification = 200 × ) (B) After 6 and 24 h of infection, the cells were fixed and double stained with rabbit anti-nestin (green) and mouse anti-3D (red) antibodies. FITC-conjugated anti-rabbit and PE conjugated anti-mouse secondary antibodies were applied for detection (magnification = 200 × ). The white arrows indicate the double positive cells with shrinkage morphology. (C) Comparison of the percentages of EV71 4643 and EV71 4643 MP4 infected NPCs. The percentage of infection was measured by dividing the number of EV71 infected cells with total number of cells in five fields.

strain, whereas cell detachment was more pronounced after 24 h of virus infection (Fig. 2A). In addition, we tested the susceptibility of mouse fibroblast 3T3 cells to EV71 infection. Similarly, the mouse-adapted 4643 MP4 strain, but not the EV71 4643 strain, caused cytopathic effects (CPE) in these cells (Fig. 2A). However, the CPE in the 3T3 cells was less apparent when compared with the NPCs. Our data demonstrated that the mouse-adapted EV71 strain caused more apparent CPE in the NPCs than in the 3T3 cells. This finding may be explained by the adaptation procedures that were performed when collecting and isolating the adapted virus from mouse brain tissue (Chen et al., 2004). To further confirm the presence of EV71 infection, immunofluorescence staining was performed to detect the EV71 3D protein in infected cells (Fig. 2B). Infected cells displayed shrinkage morphologies, including condensed nuclei (as indicated by arrows in Fig. 2B). The infected cells were counted according to the immunofluorescence staining results. In contrast to

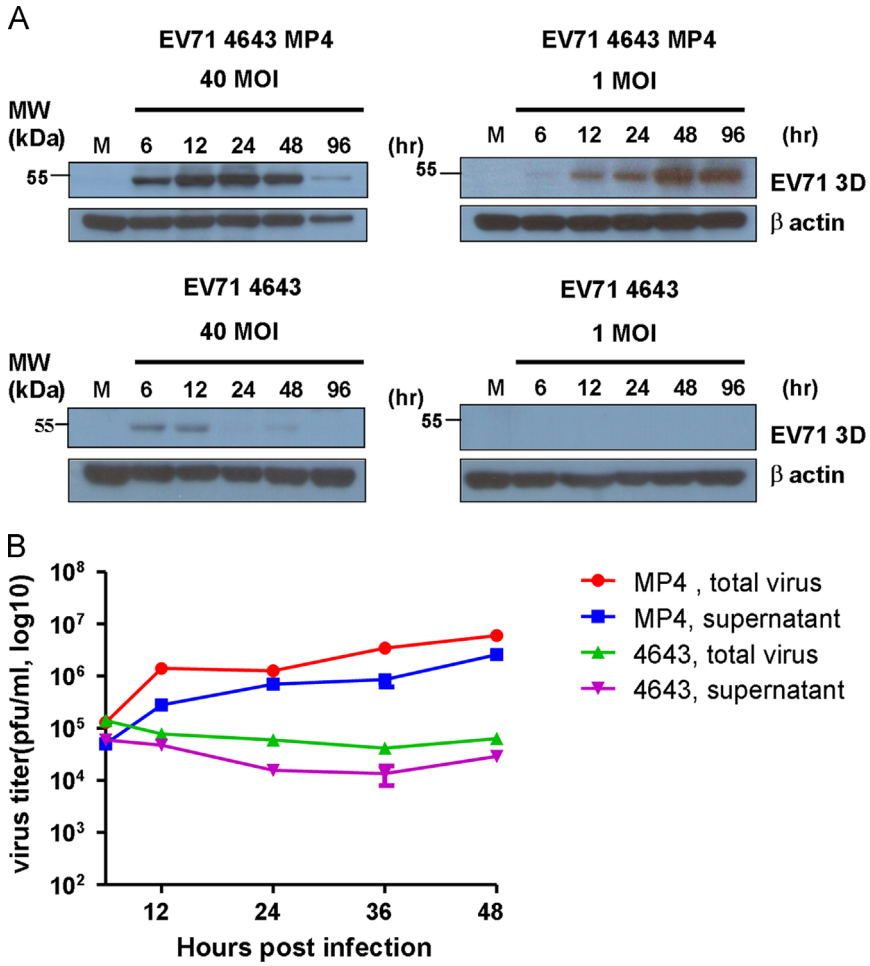


**Fig. 3.** EV71 4643 MP4 was actively replicated in mNPCs. (A) NPCs were infected with EV71 4643 MP4 or EV71 4643 at MOI of 40 or 1. After 6, 12, 24, 48 and 96 h of infection, cells were harvested for protein isolation. The proteins were then analyzed by SDS-PAGE, followed by immunoblotting with mouse anti-EV71 3D antibody. Mouse anti-β actin was used as an internal control. M: mock. (B) Viral growth curves of EV71 4643 and mouse-adapted EV71 4643 MP4 in NPCs. The titers and error bars are the means ± stdev of duplicate examples.

the EV71 4643 MP4 strain, the percentage of cells that were infected by the EV71 4643 strain did not increase over time (Fig. 2C).

*NPCs support the replication of mouse brain-adapted EV71*

To detect the expression levels of viral proteins in infected NPCs, total cell lysates were subjected to western blot analysis (Fig. 3A). The EV71 3D protein could be detected as early as 6 h post-infection (p.i.), and the protein levels peaked at 12 h in the cells that were infected with the EV71 4643 MP4 strain. Compared to the parental EV71 4643 virus, the EV71 4643 MP4 virus was induced in higher viral protein expression levels in infected NPCs. When NPCs were infected with the EV71 4643 strain at an MOI of 1, the EV71 3D protein was not detected by western blotting. The results confirmed that NPCs were more susceptible to the EV71 4643 MP4 strain. The titers of viable viral particles in the total lysates and culture supernatants were quantified using plaque assays. A one-step growth curve revealed that only the EV71 4643 MP4 strain could actively replicate in NPCs (Fig. 3B). The EV71 4643 strain infected several NPCs at a high MOI; however, these cells could not support the replication of this virus strain.

*Viral entry plays an important role in the infectivity of the EV71 4643 MP4 strain*

Previous reports indicated that receptor expression plays an important role in the permissiveness of 3T3 cells to EV71 infection (Lin et al., 2012). To test whether viral entry plays a key role in the susceptibilities of 3T3 cells and NPCs to the mouse-adapted EV71 4643 MP4 strain and the clinical isolate EV71 4643, viral RNA was isolated from both strains and transfected into NPCs. Viral protein expression levels were assessed by western blot and were similar for the two strains (Fig. 4A). These results differed from the data that we obtained from the infection assay (Fig. 3A). In addition, similar results were observed in mouse 3T3 cells. EV71 3D protein expression was absent in the 3T3 cells that were infected with the clinical isolate, EV71 4643 (Fig. 4B). However, after transfection with the EV71 4643 RNA genome, significant CPE was observed (Fig. 4C). Furthermore, the western blot analysis confirmed the expression of the viral protein (Fig. 4D). We observed that after 48 h of infection, the CPE was not as apparent as it was at 24 h post-transfection. Compared with the samples that were collected 24 h after transfection, EV71 3D protein expression was decreased at 48 h post-transfection. These results indicated that the released virions could not infect the cells, and the untransfected cells continued growing. Only traces of the EV71 3D protein could be detected in the samples that were collected 48 h after transfection. Therefore, the viral entry step plays an essential role in the infectivity of these two viruses in the tested mouse cells.

*Permissiveness of NPC-derived progenies to EV71 infection*

To test the susceptibility of differentiated neural lineage cells to EV71, the NPCs were treated to induce cell differentiation into

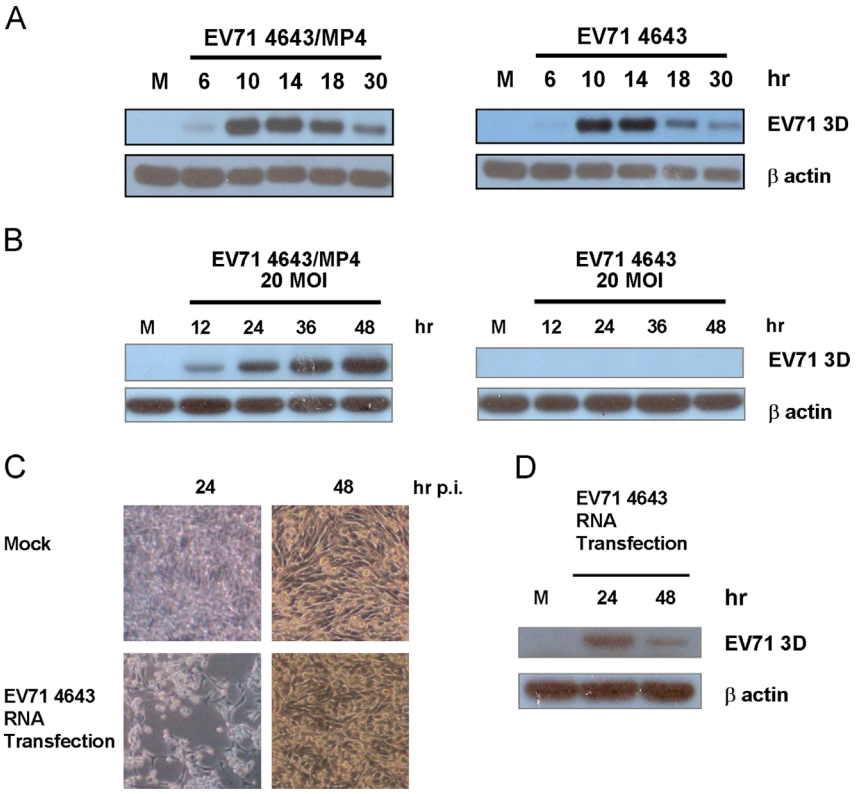


**Fig. 4.** Virus entry plays an important role in determining the permissiveness of NPCs and 3T3 cells to EV71 infection. (A) RNAs isolated from EV71 4643 and EV71 4643 MP4 were transfected into NPCs. After transfection for 6, 10, 14, 18, and 30 h, total protein was isolated from mock and virus infected cells. Western blot assay was then performed to detect the changes of EV71 3D proteins. (B) 3T3 cells were infected with EV71 4643 or EV71 4643 MP4 at an M.O.I. of 20. Total protein was extracted from cells collected at different time points. Western blot analysis was performed to examine the expression levels of EV71 3D protein. (C) Cytopathic effects were observed in 3T3 cells transfected with EV71 4643 RNA for 24 h (Magnification = 200 ×). (D) The proteins isolated from EV71 4643 RNA transfected 3T3 cells were analyzed by western blot to detect the expression levels of EV71 viral proteins.

neuronal and astrocytic progenies. The differentiated cells were confirmed by the presence of MAP2 and GFAP, which have frequently been used to identify differentiated neurons and astrocytes in stem cell research. The clinically isolated EV71 4643 strain and the mouse-adapted EV71 4643 MP4 strain were used to infect the differentiated cells, and the morphologies of the infected cells were observed and recorded. However, no obvious CPE was observed in these cells, excluding the NPCs. The possible reasons for the lack of CPE include the possibilities that these cells are not susceptible to EV71 infection and that these cells can be infected with EV71 but are resistant to EV71-triggered cell death. To confirm these hypotheses, double immunofluorescence staining was performed (Fig. 5A). Plaque assays were performed to detect the viral growth curves in the differentiated cells (Fig. 5B). The results showed that the number of viable viral particles did not increase. This could be expected because a very few differentiated cells were infected.

### *EV71 infection results in apoptosis in NPCs*

EV71 infection causes apoptosis in various cell types. To test whether the infected cells underwent apoptosis, a terminal deoxynucleotidyl transferase dUTP nick end-labeling (TUNEL) assay was performed. The EV71 4643 MP4-infected cells were positive for DNA fragmentation (Fig. 6A). Subsequently, we performed a double fluorescence immunostaining assay that revealed that most of the EV71-infected cells reacted with an anti-active caspase 3 Ab (Fig. 6B). The active caspase 3 can be detected after 12 h of infection (Fig. 6C). Thereafter, apoptosis was triggered in NPCs in response to EV71 infection. To further analyze whether other caspases are involved, anti- caspase 8 and anti- caspase 9 antibodies were used. However, our results showed that neither caspase 8 nor caspase 9 was cleaved in EV71 infected NPCs (Fig. 6D and E).

## Discussion

In this study, we showed that EV71 is able to infect NPCs both *in vivo* and *in vitro*. NPCs can differentiate into various neural lineage cells and thus play a key role in neurodevelopment. Recent studies demonstrated that the impaired function of NPCs is associated with several neurological disorders, such as Alzheimer's disease and Niemann–Pick type C disease (Verret et al., 2007; Haughey et al., 2002; Kim et al., 2008). The symptoms of these diseases include cognitive decline, learning disabilities and memory loss. In most cases, EV71-associated neurological lesions are reversible and may be resolved without sequelae. However, recent follow-up studies revealed that several patients with EV71 infection suffered from long-term complications, such as cognitive deficits (Chang et al., 2007; Huang et al., 2006). Thus, the permissiveness of NPCs to EV71 infection may explain why some long-term neurological lesions appeared.

In our study, EV71-infected cells were observed in the lining of the lateral ventricle, the SVZ, and the hippocampus, which are areas rich in NPCs (Doetsch et al., 1999). Previous studies have shown that cells infected with Coxsackievirus B3 (CVB3), a virus that preferentially targets NPCs, are primarily located in the choroid plexus, the lining of the ventricles, and the olfactory bulb (Tsueng et al., 2011; Feuer et al., 2003). Furthermore, JEV tends to infect NPCs residing in the SVZ of the fetal mouse brain (Das and Basu, 2008). These observations suggest that NPCs can serve as host cells for many different viruses. However, we did not find any EV71-infected cells

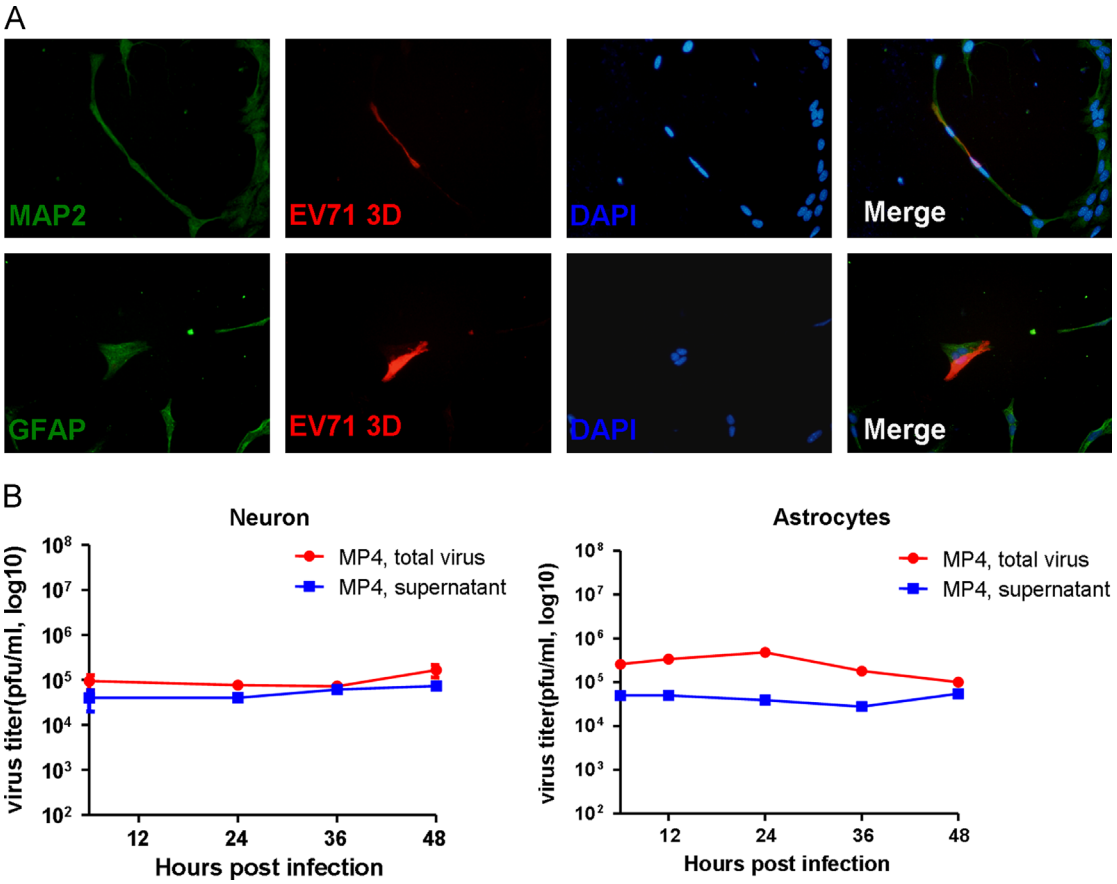


**Fig. 5.** EV71 infection of NPC-derived astrocytes and neurons. (A) NPCs were differentiated into astrocytes and neurons, and then infected by EV71 4643 MP4 at an M.O.I. of 40. The infected cells were harvested at 6 h post-infection, and stained by rabbit anti- GFAP or rabbit anti-MAP2 Abs, respectively. Anti-EV71 3D Abs were used to detect the EV71 infected cells. (magnification=200 ×). (B) Supernatants and total cell lysates were collected from EV71 4643 MP4 infected cells at different time points. Plaque assay was performed to examine the viral growth curves in differentiated cells. The titers and error bars are the means+stdev of duplicate examples.

in the olfactory bulb, most likely because the NPCs in the olfactory bulb lack EV71 receptors or because the virus particles cannot traffic to this area.

Dispersed EV71-infected neurons were detected in the cortex and the hypothalamus. However, there was no obvious difference in the numbers of infected neurons between days 1 and 2. These observations differ from those made with CVB3, which infected increasing number of neurons as the infection progressed (Feuer et al., 2003). One reason for these differences can be that the NPCs die quickly after EV71 infection while CVB3-infected NPCs can survive after infection and retain this virus even after neuronal differentiation (Tsueng et al., 2011). Another possible explanation is that the neurons may not be easily infected by EV71. Therefore, EV71 cannot efficiently infect neuronal cells, and the number of infected neurons do not increase over time.

Viral infections of NPCs could interfere with normal cell function and alter cell fate. Neurotrophic viruses, such as JEV, human cytomegalovirus (HCMV), and BDV, can infect NPCs (Das and Basu, 2008; McCarthy et al., 2000; Brnic et al., 2012). JEV infects neural stem cells (NSCs) and impairs neural progenitor division, which may be associated with long-term cognitive deficits in survivors (Das and Basu, 2008). Furthermore, BDV-infected neural progenitors cannot generate neuronal progeny, which may lead to impaired neural function and behavioral disorders (Brnic et al., 2012). Our results showed that active caspase 3 colocalized with EV71-infected NPCs, suggesting that EV71 infection is associated with apoptosis. EV71 infection led to the activation of caspase 8 and 9 in RD cells (Shi et al., 2012; Wang et al., 2012). Infection with EV71 induces the cleavage of caspase 9 activation in all tested cells including SK-N-SH (human neuroblastoma), SK-N-MC (human neuroblastoma), SF268 (human glioblastoma), Caco-2 (colon carcinoma) and Vero cells. In contrast, the activation of caspase 8 is observed in EV71 infected non-neural cells (Wang et al., 2004; Chang et al., 2004). However, neither caspase 8 or caspase 9 was activated in EV71-infected NPCs. Therefore, we speculated that EV71 may activate caspase 3 without cleaving caspase 8 and caspase 9. We have previously studied EV71-induced apoptosis in SF268 cells, a human glioblastoma cell line. We found that viral protein synthesis is essential for EV71 infection-induced apoptosis (Shih et al., 2008.) In this study, our results revealed that active caspase 3 was only detected in cells that were positive for the EV71 viral protein, which was in accordance with our previous observations. The EV71 2A and 3C proteins possess proteolytic activities that trigger the caspase cascade (Li et al., 2002; Kuo et al., 2002). However, we have not identified which viral protein is essential for the induction of apoptosis in NPCs.

We tested the susceptibility of NPC-derived neuronal and astrocytic progenies to EV71 infection. The results indicated that a few cells could be infected by the EV71. These cells were less susceptible to EV71 infection when compared with undifferentiated NPCs most likely because the differentiated neuronal and astrocytic cells were deficient for appropriate EV71 receptors or because these cells lacked essential factors for efficient EV71 translation and replication. EV71, like some other neurotrophic viruses, tends to infect children (Drăgănescu et al., 1980; Ogata et al., 1991). Unlike adults, the brains of children are still developing and may contain more EV71-susceptible cells. Previous research has demonstrated that CVB3 preferentially replicates in actively proliferating cells (Feuer et al., 2002; Luo et al., 2003). Additional experimental evidence is needed to determine whether

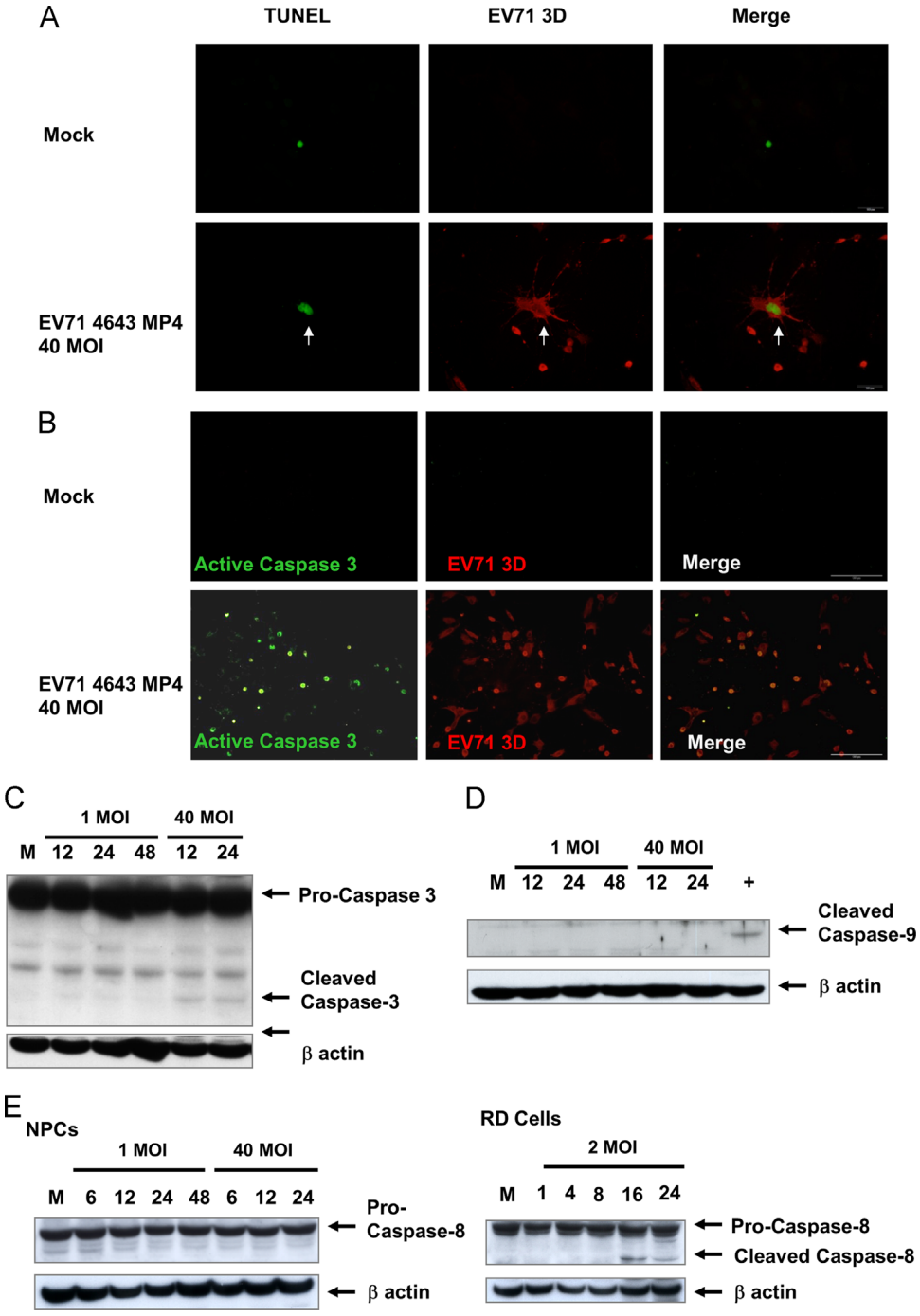


**Fig. 6.** EV71 infection triggers apoptosis in NPCs. (A) To detect the DNA fragmentation, TUNEL assay was performed. NPCs infected by EV71 4643 MP4 were fixed after 24 h of infection. The positive staining cells were shown with green fluorescence in the cell nucleus. EV71 infection was confirmed by stained with EV71 3D antibodies. The white arrow indicated the EV71 infected NPC which was also positive for DNA fragmentation (Magnification = 200 ×). (B) NPCs were infected with EV71 4643 MP4 at an M.O.I. of 40 for 24 h, cells were then fixed for double-immunoflorescence staining assay. After fixation, cells were allowed to react with anti-active caspase 3 Ab first, FITC-conjugated anti-rabbit IgG secondary Ab was then applied to detect the signals. Thereafter, anti-EV71 3D Ab was used to detect the cells infected by EV71, PE-conjugated anti-mouse IgG Abs were applied for detection. (Magnification = 200 ×) (C) Western blot was performed to detect the expression of active caspase 3 in EV71 infected NPCs. β-actin was used as an internal control. (D) The cleaved form of caspase 9 was determined by western blot. EV71 (2 MOI) infected RD cell lysate (16 h p.i.) was used as positive control. (E) Total lysates were collected from EV71 infected NPCs and RD cells and were applied for western blot analysis to detect the cleaved caspase 8.

the different susceptibilities of undifferentiated and differentiated NPCs to EV71 infection are associated with active cell proliferation. Therefore, in addition to viral receptors, the status of host cells may contribute to the different susceptibilities of NPCs and other neural lineage cells to EV71 infection.

In a previous study, EV71 proteins could be detected in the brain neurons of infected patients and animals (Chan et al., 2000). However, the types of infected neurons were not yet identified. A possible explanation for why so few NPC-derived neuronal cells were infected by EV71 is the heterogeneity of neuronal populations. The brain contains many different types of neurons, such as motor neurons, sensory neurons, and Purkinje cells. These neuronal populations possess diverse properties and may have differential susceptibilities to specific viruses. For example, Varicella-zoster virus (VZV) tends to

infect sensory neurons, whereas HIV invades neocortical neurons (Lee et al., 2012; Fisher et al., 1999). However, further studies should be performed to identify the types of neurons that are more permissive to EV71 infection.

The data from this study demonstrated that NPCs are permissive to EV71 infection and that these cells support active viral replication. However, NPC-derived neurons and glial cells were less susceptible to EV71. EV71 infection results in the apoptosis of infected NPCs, which may lead to the loss of the NPC pool in the CNS. In conclusion, the data from this study provide insights into the permissiveness of neural lineage cells to EV71 infection and demonstrate that NPCs may serve as a reservoir for EV71 in the CNS.

## Materials and methods

### *Cells and virus*

Mouse brain-derived neural progenitor cells (mNPCs) were cultured in alpha minimum essential medium (α-MEM, Gibco-Invitrogen, CA, USA) supplemented with 10% fetal bovine serum (FBS). A human rhabdomyosarcoma (RD) cells line was cultured in Dulbecco's Modified Eagle Medium (DMEM) supplemented with 10% fetal bovine serum (FBS), 1% L-Glutamine, 1% non-essential amino acid, and 1X penicillin/streptomycin (P/S) (all from Gibco-Invitrogen, CA, USA). Cells were maintained in a 37 °C incubator equilibrated with 5% $CO_2$. The clinically isolated strains of Enterovirus 71 strain 4643 (TW/Tainan/4643/98) and mouse adaptive EV71 4643 MP4 (EV71/Tainan/4643/98 MP4) (kindly provided by Prof. Jen-Ren Wang at National Cheng-Kung Hospital) were amplified in RD cells that were cultured in DMEM supplemented with 2% FBS and 1X P/S. The titer of the virus stocks was measured using plaque-forming assay and the number of plaque-forming units (pfu) was calculated.

### *Virus infection*

Cells ($10^5$/well) were seeded in 12-well plates for approximately 16 h before infection. After washed twice with phosphate buffered saline (PBS), viruses were added to the wells at a specified multiplicity of infection (M.O.I.) in serum-free culture medium for 1 h at 37 °C. After 1 h of adsorption, the cells were washed twice with PBS to remove unbound viruses and replaced with 1 ml of fresh α-MEM containing 2% FBS per well. The cell morphology was monitored and recorded using an optical microscope at different time points.

### *Western blot*

The cultured cells were washed with PBS, and the total cell lysates were collected using an ice-cold protein lysis buffer (1% NP-40, 50 mM Tris, and 150 mM NaCl) supplemented with protease inhibitors cocktail, and incubated on ice for 30 min. After centrifugation at 13,000 r.p.m. for 10 min at 4 °C, the supernatant and pellet fractions were collected. Protein concentrations were measured using the Bradford method (Bio-Rad Laboratories, CA, USA), and 30 μg of protein was separated by 10% SDS-polyacrylamide gel electrophoresis, and then transferred onto a polyvinylidene fluoride membrane (PVDF) ( Millipore, Billerica, MA, USA). The membrane was blocked with 5% skim milk in Tris-buffered saline Tween-20 buffer (TBST) at room temperature (20 mmol/L Tris–HCl, pH 7.4, 150 mmol/L NaCl, and 0.1% Tween 20). The membrane was then incubated with anti-EV71 3D antibody (1:10,000), anti-active caspase 3, anti-caspase 8 (both from Cell Signaling, 1:1000), anti-caspae 9 (Santa Cruz, 1:1000) or β-actin (Sigma-Aldrich, Missouri, U.S.A., 1:20,000), and probed with horseradish peroxidase conjugated anti-mouse secondary antibody (Jackson ImmunoResearch Laboratories, Pennsylvania, U.S.A., 1:5000). The target proteins were then visualized in a subsequent chemiluminescence reaction (Thermo Scientific, Illinois, U.S.A.).

### *Neuronal and astrocytic differentiation*

For neural differentiation, NPCs ($10^5$ cells per well) were plated on 12-well plates coated with poly-L-Lysine (Sigma-Aldrich) in α-MEM supplemented with 10%FBS. After 1 day, the medium was removed, and the cells were washed twice with PBS and cultured in serum-free α-MEM. The cells were incubated at 37 °C in 5% $CO_2$ for 14 days, and immunofluorescence staining (primary antibody: rabbit anti-MAP2, secondary antibody: goat anti-rabbit Dylight488) was used to confirm the differentiation. To induce astrocytes differentiation, NPCs ($10^5$ cells /well) were plated on 12-well plates. After 1 day, the medium was removed, and the cells were washed twice with PBS and cultured in serum-free α-MEM containing 3-isobutyl-1-methylxanthine (IBMX, 0.1 mM). The cells were incubated at 37 °C in 5% $CO_2$ for 3 days, and IFA (primary antibody: rabbit anti-GFAP, secondary antibody: goat anti-rabbit Dylight488) was used to confirm the differentiation.

### *Immunofluorescence assay*

The NPCs-differentiated neurons or astrocytes infected with clinical isolate strain EV71/Tainan/4643/98 (EV71) or mouse adaptive strain EV71/Tainan/4643/98 MP4 (EV71 MA) at M.O.I. of 40 were collected at 6 h and 24 h post-infection, and washed once by PBS. The cells were then fixed with ice-cold fixative solution (ethanol–methanol, 1:1) for 1 min, and then blocked with 0.5% FBS in PBS for 30 min at room temperature. The cells were incubated overnight at 4 °C with primary antibodies, rabbit anti-nestin (Santa Cruz Biotechnology, California, U.S.A., 1:50), rabbit anti-MAP2(Millipore, 1:200), rabbit anti-GFAP(Millipore, 1:200) and mouse anti-EV71 3D (1:800). After washed twice with PBS , the cells were then probed with DyLight 488-conjugated anti-rabbit secondary antibodies (Jackson ImmunoResearch Laboratories, Pennsylvania, U.S.A., 1:800) or Dylight594 conjugated donkey anti-mouse antibodies (Jackson ImmunoResearch Laboratories, Pennsylvania, U.S.A., 1:800). After incubation at room temperature for 1 h, cells were washed twice with PBS. The cell nuclei were stained with DAPI (1:10,000) for 5 min. The results were examined under a fluorescence microscope system (Olympus).

### *Plaque assay*

The RD cells were seeded in 6-well plates ($5.5 \times 10^5$ cells per well), incubated at 37 °C in 5% $CO_2$ for 20–24 h. The cells were then washed once with PBS and infected with 500 μl of serially diluted virus suspensions in a serum-free medium. After 1 h of adsorption at 37 °C in 5% $CO_2$, the culture media was removed and the cells were washed twice with PBS to remove unbound viruses. Afterward 3 ml of MEM containing 2% FBS and 0.3% agarose gel was added to each well. After 4 days, the cells were fixed with 10% formaldehyde for more than 1 h and subsequently stained with crystal violet solution. The titer of the virus was expressed as pfu/ml.

### *Animal experiment*

The animal protocols were approved by the Institutional Animal Care and Use Committee of Chang Gung University. Imprinting Control Region (ICR) mice were obtained from Lasco Biotechnology Company (Taipei, Taiwan). 5-day-old mouse were injected intraperitoneally with $5 \times 10^5$ pfu of EV71/Tainan/4643/98 MP4 per mice.

Control mice were injected with culture medium. After 24 and 48 h of injection, the animals were sacrificed and the brain tissue samples were collected for further analysis ($n=5$ for each infected group and $n=4$ for each mock infected group).

## Acknowledgments

This work is supported by Grant NSC-99-2321-B-002-025 from National Science Council Taiwan and Grants CMRPD 190253 and CMRPD1C0602 from Chang Gung Memorial Hospital.

## Appendix A. Supporting information

Supplementary data associated with this article can be found in the online version at http://dx.doi.org/10.1016/j.virol.2014.09.017.

## References

Ariff, I.M., Thounaojam, M.C., Das, S., Basu, A., 2013. Japanese encephalitis virus infection alters both neuronal and astrocytic differentiation of neural stem/progenitor cells. J. Neuroimmune Pharmacol. 8, 664–676.
Brnic, D., Stevanovic, V., Cochet, M., Agier, C., Richardson, J., Montero-Menei, C.N., Milhavet, O., Eloit, M., Coulpier, M., 2012. Borna disease virus infects human neural progenitor cells and impairs neurogenesis. J. Virol. 86, 2512–2522.
Briese, T., Hornig, M., Lipkin, W.I., 1999. Bornavirus immunopathogenesis in rodents: models for human neurological diseases. J. Neurovirol. 5, 604–612.
Chan, L.G., Parashar, U.D., Lye, M.S., Ong, F.G., Zaki, S.R., Alexander, J.P., Ho, K.K., Han, L.L., Pallansch, M.A., Suleiman, A.B., Jegathesan, M., Anderson, L.J., 2000. Deaths of children during an outbreak of hand, foot, and mouth disease in sarawak, malaysia: clinical and pathological characteristics of the disease. For the Outbreak Study Group. Clin. Infect. Dis. 31, 678–683.
Chang, L.Y., King, C.C., Hsu, K.H., Ning, H.C., Tsao, K.C., Li, C.C., Huang, Y.C., Shih, S.R., Chiou, S.T., Chen, P.Y., Chang, H.J., Lin, T.Y., 2002. Risk factors of enterovirus 71 infection and associated hand, foot, and mouth disease/herpangina in children during an epidemic in Taiwan. Pediatrics 109, e88.
Chang, L.Y., Huang, L.M., Gau, S.S., Wu, Y.Y., Hsia, S.H., Fan, T.Y., Lin, K.L., Huang, Y.C., Lu, C.Y., Lin, T.Y., 2007. Neurodevelopment and cognition in children after enterovirus 71 infection. N. Engl. J. Med. 356, 1226–1234.
Chang, S.C., Lin, J.Y., Lo, L.Y., Li, M.L., Shih, S.R., 2004. Diverse apoptotic pathways in enterovirus 71-infected cells. J. Neurovirol. 10, 338–349.
Cheeran, M.C., Hu, S., Ni, H.T., Sheng, W., Palmquist, J.M., Peterson, P.K., Lokensgard, J.R., 2005. Neural precursor cell susceptibility to human cytomegalovirus diverges along glial or neuronal differentiation pathways. Neurosci. Res. 82, 839–850.
Chen, C.Y., Chang, Y.C., Huang, C.C., Lui, C.C., Lee, K.W., Huang, S.C., 2001. Acute flaccid paralysis in infants and young children with enterovirus 71 infection: MR imaging findings and clinical correlates. AJNR: Am. J. Neuroradiol. 22, 200–205.
Chen, Y.C., Yu, C.K., Wang, Y.F., Liu, C.C., Su, I.J., Lei, H.Y., 2004. A murine oral enterovirus 71 infection model with central nervous system involvement. J. Gen. Virol. 85, 69–77.
Das, S., Basu, A., 2008. Japanese encephalitis virus infects neural progenitor cells and decreases their proliferation. J. Neurochem. 106, 1624–1636.
Doetsch, F., Caille, I., Lim, D.A., Garcia-Verdugo, J.M., Alvarez- Buylla, A., 1999. Subventricular zone astrocytes are neural stem cells in the adult mammalian brain. Cell 97, 703–716.
Drăgănescu, N., Nereanţiu, F., Girjabu, E., 1980. Coxsackie B2 virus isolation from a case of postnatal meningoencephalitis. Virologie 31, 9–12.
Feuer, R., Mena, I., Pagarigan, R., Slifka, M.K., Whitton, J.L., 2002. Cell cycle status affects coxsackievirus replication, persistence, and reactivation in vitro. J. Virol. 76, 4430–4440.
Feuer, R., Mena, I., Pagarigan, R.R., Harkins, S., Hassett, D.E., Whitton, J.L., 2003. Coxsackievirus B3 and the neonatal CNS: the roles of stem cells, developing neurons, and apoptosis in infection, viral dissemination, and disease. Am. J. Pathol. 163, 1379–1393.
Fisher, C.P., Jorgen, G., Gundersen, H., Pakkenberg, B., 1999. Preferential loss of large neocortical neurons during HIV infection: a study of the size distribution of neocortical neurons in the human brain. Brain Res. 828, 119–126.
Haughey, N.J., Liu, D., Nath, A., Borchard, A.C., Mattson, M.P., 2002. Disruption of neurogenesis in the subventricular zone of adult mice, and in human cortical neuronal precursor cells in culture, by amyloid beta-peptide: implications for the pathogenesis of Alzheimer's disease. Neuromol. Med. 1, 125–135.
Hofer, S., Grandgirard, D., Burri, D., Frohlich, T.K., Leib, S.L., 2011. Bacterial meningitis impairs hippocampal neurogenesis. J. Neuropathol. Exp. Neurol. 70, 890–899.
Huang, M.C., Wang, S.M., Hsu, Y.W., Lin, H.C., Chi, C.Y., Liu, C.C., 2006. Long-term cognitive and motor deficits after enterovirus 71 brainstem encephalitis in children. Pediatrics 118, e1785–8.
Kim, S.J., Park, J.S., Kang, K.S., 2008. Stem cells in Niemann–Pick disease. Dis. Markers 24, 231–238.
Kuo, R.L., Kung, S.H., Hsu, Y.Y., Liu, W.T., 2002. Infection with enterovirus 71 or expression of its 2A protease induces apoptotic cell death. J. Gen. Virol. 83 (Pt. 6), 1367–1376.
Lee, K.S., Zhou, W., Scott-McKean, J.J., Emmerling, K.L., Cai, G.Y., Krah, D.L., Costa, A.C., Freed, C.R., Levin, M.J., 2012. Human sensory neurons derived from induced pluripotent stem cells support varicella-zoster virus infection. PLoS One 7, e53010.
Lendahl, U., Zimmerman, L.B., McKay, R.D., 1990. CNS stem cells express a new class of intermediate filament protein. Cell 60, 585–595.
Li, M.L., Hsu, T.A., Chen, T.C., Chang, S.C., Lee, J.C., Chen, C.C., Stollar, V., Shih, S.R., 2002. The 3C protease activity of enterovirus 71 induces human neural cell apoptosis. Virology 293, 338–349.
Lin, Y.W., Lin, H.Y., Tsou, Y.L., Chitra, E., Hsiao, K.N., Shao, H.Y., Liu, C.C., Sia, C., Chong, P., Chow, Y.H., 2012. Human SCARB2-mediated entry and endocytosis of EV71. PLoS One 7, e30507.
Luo, H., Zhang, J., Dastvan, F., Yanagawa, B., Reidy, M.A., Zhang, H.M., Yang, D., Wilson, J.E., McManus, B.M., 2003. Ubiquitin-dependent proteolysis of cyclin D1 is associated with coxsackievirus-induced cell growth arrest. J. Virol. 77, 1–9.
McCarthy, M., Auger, D., Whittemore, S.R., 2000. Human cytomegalovirus causes productive infection and neuronal injury in differentiating fetal human central nervous system neuroepithelial precursor cells. J. Hum. Virol. 3, 215–228.
McKay, R., 1997. Stem cells in the central nervous system. Science 276, 66.
McMinn, P.C., 2002. An overview of the evolution of enterovirus 71 and its clinical and public health significance. FEMS Microbiol. Rev. 26, 91–107.
Melnick, J.L., 1984. Enterovirus type 71 infections: a varied clinical pattern sometimes mimicking paralytic poliomyelitis. Rev. Infect. Dis. 6 (Suppl. 2), S387–390.
Odeberg, J., Wolmer, N., Falci, S., Westgren, M., Seiger, A., Söderberg-Nauclér, C., 2006. Human cytomegalovirus inhibits neuronal Differentiation and induces apoptosis in human neural precursor cells. J. Virol. 80, 8929–8939.
Odeberg, J., Wolmer, N., Falci, S., Westgren, M., Sundtröm, E., Seiger, A., Söderberg-Nauclér, C., 2007. Late human cytomegalovirus (HCMV) proteins inhibit differentiation of human neural precursor cells into astrocytes. J. Neurosci. Res. 85, 583–593.
Ogata, A., Nagashima, K., Hall, W.W., Ichikawa, M., Kimura-Kuroda, J., Yasui, K., 1991. Japanese encephalitis virus neurotropism is dependent on the degree of neuronal maturity. J. Virol. 65, 880–886.
Schmidt, N.J., Lennette, E.H., Ho, H.H., 1974. An apparently new enterovirus isolated from patients with disease of the central nervous system. J. Infect. Dis. 129, 304–309.
Shi, W., Li, X., Hou, X., Peng, H., Jiang, Q., Shi, M., Ji, Y., Liu, X., Liu, J., 2012. Differential apoptosis gene expressions of rhabdomyosarcoma cells in response to enterovirus 71 infection. BMC Infect. Dis. 12, 327.
Shih, S.R., Weng, K.F., Stollar, V., Li, M.L., 2008. Viral protein synthesis is required for enterovirus 71 to induce apoptosis in human glioblastoma cells. J. Neurovirol. 14, 53–61.
Su, K., de Vellis, J., 2009. Stem cell-based cell therapy in neurological diseases: a review. J. Neurosci. Res. 87, 2183–2200.
Tsueng, G., Tabor-Godwin, J.M., Gopal, A., Ruller, C.M., Deline, S., An, N., Frausto, R.F., Milner, R., Crocker, S.J., Whitton, J.L., Feuer, R., 2011. Coxsackievirus preferentially replicates and induces cytopathic effects in undifferentiated neural progenitor cells. J. Virol. 85, 5718–5732.
Verret, L., Jankowsky, J.L., Xu, G.M., Borchelt, D.R., Rampon, C., 2007. Alzheimer's-type amyloidosis in transgenic mice impairs survival of newborn neurons derived from adult hippocampal neurogenesis. J. Neurosci. 27, 6771–6780.
Wang, C.Y., Huang, S.C., Zhang, Y., Lai, Z.R., Kung, S.H., Chang, Y.S., Lin, C.W., 2012. Antiviral ability of Kalanchoe gracilis leaf extract against enterovirus 71 and coxsackievirus A16. Evid. Based Complement. Altern. Med., 503165.
Wang, S.M., Liu, C.C., Tseng, H.W., Wang, J.R., Huang, C.C., Chen, Y.J., Yang, Y.J., Lin, S.J., Yeh, T.F., 1999. Clinical spectrum of enterovirus 71 infection in children in southern Taiwan, with an emphasis on neurological complications. Clin. Infect. Dis. 29, 184–190.
Wang, Y.F., Chou, C.T., Lei, H.Y., Liu, C.C., Wang, S.M., Yan, J.J., Su, I.J., Wang, J.R., Yeh, T.M., Chen, S.H., Yu, C.K., 2004. A mouse-adapted enterovirus 71 strain causes neurological disease in mice after oral infection. J. Virol. 78, 7916–7924.
Wang, S.M., Ho, T.S., Lin, H.C., Lei, H.Y., Wang, J.R., Liu, C.C., 2011. Reemerging of enterovirus 71 in Taiwan: the age impact on disease severity. Eur. J. Clin. Microbiol. Infect. Dis. 31, 1219–1924.